INT. COMM. HEAT MASS TRANSFER 0735-1933/86 $3.00 + .00
Vol. 13, pp. 665-674, 1986 ©Pergamon Journals Ltd. Printed in the United States

NUMERICAL SIMULATION OF HEAT TRANSFER IN THE SEPARATED AND REATTACHED FLOW ON A BLUNT FLAT PLATE

M.C. Thompson, K. Hourigan and M.C. Welsh
Commonwealth Scientific and Industrial Research Organization
Division of Energy Technology, Highett, Victoria, Australia

(Communicated by J.P. Hartnett and W.J. Minkowycz)

ABSTRACT

The time-dependent heat transfer process in the region of a turbulent separation bubble at the leading edge of an isothermal square leading edge plate is modelled numerically. A discrete-vortex model is used to determine the velocity field and a third-order upwind differencing technique is used to calculate the thermal field. The prediction of the mean Nusselt numbers is compared with experiment. The model predicts the instantaneous streamlines, isotherms and local Nusselt numbers at the plate surface. The influence of the large-scale vortex structures on the local heat transfer is determined.

Introduction

Heat transfer in separated, reattached and redeveloped flow regions is important in many engineering situations. There has been a large number of investigations carried out on such flows for a wide variety of bluff bodies. These include circular cylinders (e.g. Morgan [1]), forward and backward facing steps (e.g. Gooray et al. [2]), surface roughness elements and abrupt expansions or contractions in tubes (e.g. Sparrow and O'Brien [3]). In recent years, a number of experimental studies have been undertaken to determine the mean thermal characteristics of such flows around blunt flat plates which are heated (Ota and Kon [4], Zelenka and Loehrke [5], Cooper et al. [6], MacCormick et al. [7], Motwani et al. [8]). These measurements show that the time-mean heat transfer is augmented when the flow is made to separate and reattach. The heat transfer characteristics along the plate surface vary significantly; a local minimum in the Nusselt number is found inside the separation bubble and a local maximum near reattachment.

Recently, mechanisms involving large-scale vortex structures have been proposed to explain the enhanced heat transfer near the point of time-mean reattachment (e.g. Kiya and Sasaki [9]). A determination of the mechanisms leading to the variation of the heat transfer in different regions of the flow requires evaluation of the instantaneous flow. In this paper, an economical numerical method for investigating the influence on the heat transfer rate of the turbulent structures formed in separated high Reynolds number flows is presented. A discrete-vortex model is used to predict the high Reynolds number flow and a finite-difference scheme is used to solve the energy equation. For economy of computation, the solution obtained is restricted here to moderate Peclet numbers. However, as the flow of energy is still dominated by convection processes, valuable insights into the mechanisms leading to heat transfer augmentation are found to emerge from this type of approach.

Numerical Model

The flow considered is that past a rigid, two-dimensional, semi-infinite heated flat plate, which is aligned with a square leading edge normal to the flow. The flow upstream is taken to be of uniform velocity and temperature. The fluid is assumed to be inviscid, incompressible and irrotational everywhere except at points where simple inviscid line vortices are located. These vortices allow representation of the larger scale flow structures. Attention is focussed on the shear layer separating from the top leading edge corner. The vorticity generated at the lower leading edge corner is assumed to have negligible effect on the shear layer at the top of the plate.

Vorticity Equation: Discrete-vortex model

The continuous sheet of vorticity entering the flow from the leading edge of the plate is approximated by a distribution of line vortices. The motion of each vortex is determined through the contributions from the irrotational field, both the steady and fluctuating components, and from the vorticity field due to other line vortices. In order to satisfy the condition of zero flow across the solid plate boundary, the following Schwarz-Christoffel conformal transformation is used to locate image vortices:

$$z = (\lambda(\lambda^2 - 1)^{1/2} - \text{arcosh}\,(\lambda))\, 2H/\pi + iH \,.$$

This transformation maps the flow around a semi-infinite plate (z-plane) into the flow bounded by the real axis (λ-plane). The image vortices are placed at conjugate positions to the vortices in the upper half of the λ-plane to satisfy the boundary condition of zero normal flow. The advection of the vortices follows closely the scheme used by Kiya et al. [10]. The introduction of vorticity at the leading edge corner and determination of its strength is based on the scheme used by Nagano et al. [11].

An important innovation in the present scheme is the recognition of the mechanism leading to the generation of vorticity and of that responsible for annihilation of vorticity in the flow. That is, in a homogeneous fluid, vorticity is generated at a boundary and its rate of generation is proportional to the tangential surface pressure gradient. The presence of viscosity leads to a net flux of vorticity into the fluid at the same rate (Morton [12]). In the present model, the amount of vorticity shed into the flow along the plate is adjusted to be consistent with the pressure drop along its surface, which in turn is influenced by previously introduced vorticity. For long plates, the difference in the normalized pressure coefficient at the center of the leading edge and that downstream of reattachment is found to be approximately unity, both experimentally (e.g. Hillier and Cherry [13]) and by the present model. The scheme used here is to reduce the strengths of vortices recirculating upstream of time-mean reattachment by a fixed fraction each time-step; this fraction is determined by running the code and iteratively adjusting the fractional value until the net vorticity generation rate is consistent to within one percent of the time-mean pressure drop along the plate surface.

Energy Equation : Finite-difference approximation

The energy equation to be solved is given by

$$\partial T/\partial \tau + (\underline{u}.\text{grad})\, T = Pe^{-1}\, \text{div}\, (\text{grad}\, T)\ .$$

The velocity $\underline{u}$ is determined at each step by the discrete-vortex scheme, using a discrete approximation to the Biot-Savart integral.

The energy equation is solved using QUICKEST (Leonard [14]). This explicit scheme uses third order upstream differencing for the advection terms and includes an estimation for the truncated time difference terms in a similar manner to Leith's method [15]. The method approaches third order accuracy in both time and space as the Peclet number approaches infinity (for a constant flow velocity).

GRID AND BOUNDARY CONDITIONS

51 x 31 GRIDPOINTS

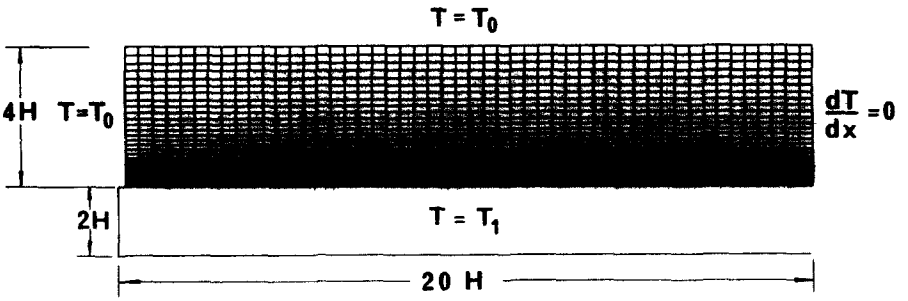

FIG. 1
Quadratically compressed mesh used for finite-difference scheme, with boundary conditions marked

To accommodate the higher temperature gradients near the plate surface, a quadratic transformation for the vertical coordinate is adopted; a compression factor of ten is used here. The mesh and boundary conditions are shown in Figure 1. For the present calculations the mesh used is 51 x 31. The time step for both the discrete-vortex method and the finite-difference scheme is 0.05 ($2H/V_\infty$). The Peclet number used is Pe = 40. The numerical code was run on a Cyber 205 computer. The (vectorized) code takes approximately 350 seconds of CPU time per 1000 timesteps.

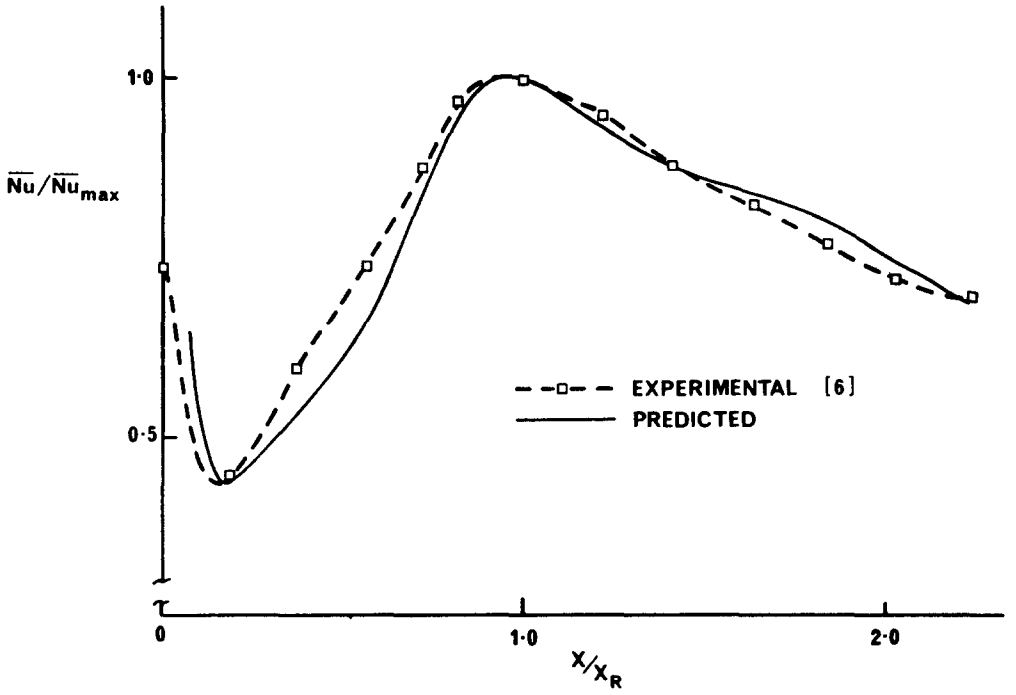

FIG. 2
Predicted and observed (Cooper et al. [6]) time-mean local Nusselt numbers along the plate surface

Results and Discussion

The time-mean Nusselt numbers at the plate surface are shown in Figure 2. The Nusselt numbers are normalized to the maximum value occurring near reattachment. The Nusselt number is at a local minimum in the separation bubble and a local maximum near reattachment; the predicted time-mean reattachment length x_R being 9.3H. The local Nusselt number decreases monotonically in the direction downstream of reattachment. For comparison, the normalized local Nusselt numbers measured by Cooper et al. [6] are shown. Although the absolute values of the Nusselt numbers are lower (due to the use of a lower Peclet number), the normalized Nusselt numbers are found to be in good agreement with the experimental results.

A typical time trace of the point of streamline reattachment is shown in Figure 3. It is seen that in general the bubble steadily grows in length until a new reattachment point forms upstream and the bubble is discontinuously shortened. This result is consistent with the experimental findings of Kiya and Sasaki [9]; these showed the continual formation of new points of zero velocity upstream of the point of mean reattachment as large-scale structures were released from the separation bubble.

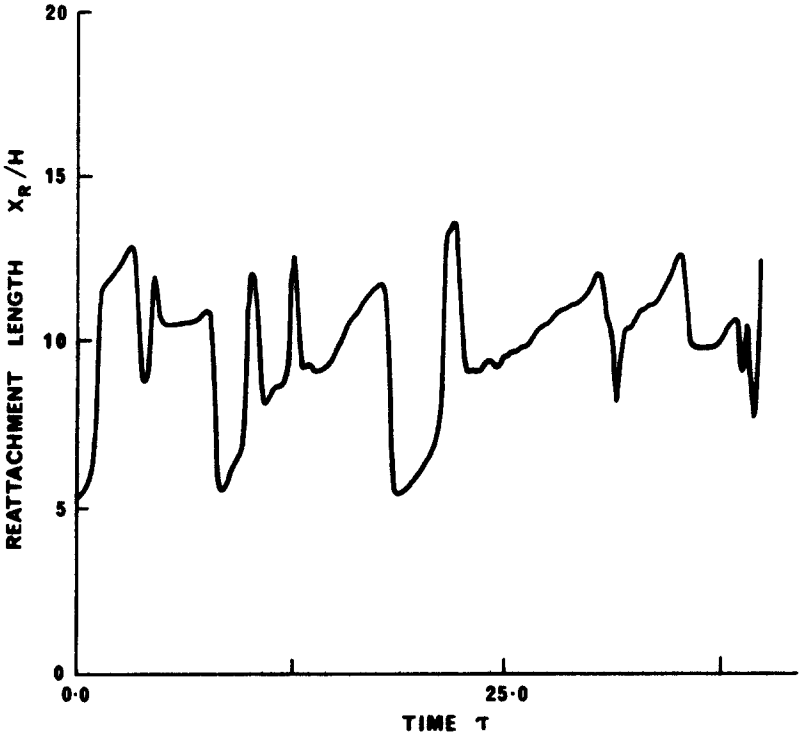

FIG. 3
Predicted time trace of the reattachment length for the flow model

A time-averaged measure of the intensity of transport of thermal energy in the vertical direction due to vortices in the flow is the vertical thermal eddy diffusivity D_v, which indicates the correlation between vertical velocity fluctuations and temperature fluctuations. This is plotted in Figure 4. The position of maximum diffusivity in the chordwise direction along the plate is found in the neighborhood of the position of maximum Nusselt number downstream of the leading edge. This result suggests that the augmentation of heat transfer results from vortex action in moving warm fluid away from the surface and cool fluid towards the heated plate.

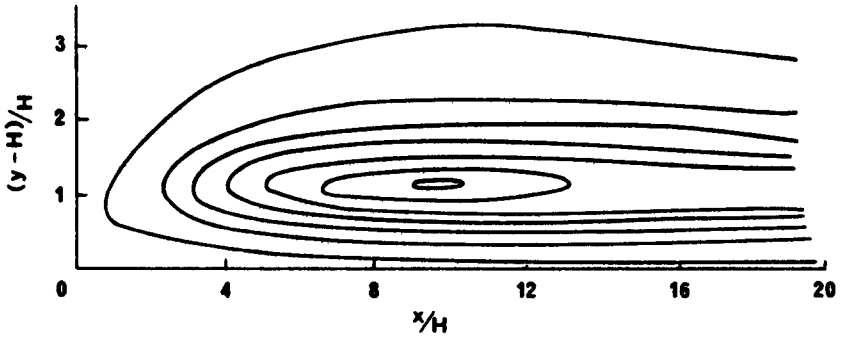

FIG. 4
Predicted contours of the vertical thermal eddy diffusivity D_v

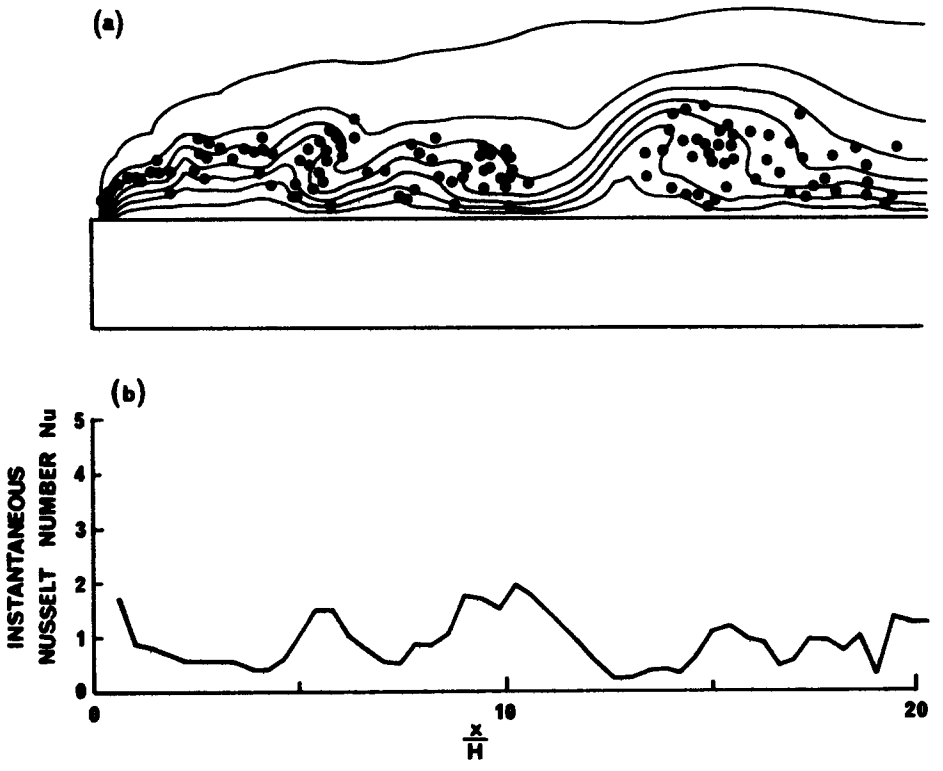

FIG. 5
Predicted snapshots of (a) instantaneous vortex positions and isotherms and (b) instantaneous local Nusselt number profile

More importantly, from the point of view of understanding the mechanisms leading to the augmented heat transfer when the flow is made to separate and reattach, are the predictions of time-dependent quantities. Characteristic instantaneous isotherms together with the vortex positions and Nusselt numbers are shown in Figure 5. The influence of the large-scale vortex structures on the local heat transfer rate is apparent. A local peak in the Nusselt number is found from this snapshot, and others not shown, to be associated with each large-scale structure. This is interpreted as the action of these structures in drawing cooler fluid towards the surface immediately downstream of the vortex positions. The fluid being drawn close to the instantaneous point of reattachment is relatively cool, having flowed over the separation bubble away from the heated surface. The relatively large temperature difference between the plate and this cooler fluid accounts for the higher heat transfer rates observed at the reattachment point. Inside the separation bubble, the recirculating flow is generally less turbulent and of lower velocity; this leads to a generally higher thermal resistance, as reflected by the lower values of both the time-mean and instantaneous Nusselt numbers in this region.

It is, perhaps, significant that the relative heat transfer characteristics along the plate surface are predicted quite well by an essentially inviscid, two-dimensional model. However, this agreement is not surprising : the findings of Rothe and Johnston [16] indicate that the spanwise vortices are primarily responsible for the region of unsteady reversing flow in the neighborhood of the mean reattachment point; the dominant vehicles of energy transport, the large-scale structures, are little influenced by viscosity, which may therefore be neglected.

Conclusions

A time-dependent model of the heat transfer process near a turbulent separation bubble has been presented. The velocity field is deduced from the vorticity field that is provided by a discrete-vortex model of the flow. The thermal field is calculated simultaneously using a third-order finite-difference approximation to solve the energy equation on a quadratically compressed grid.

The peak time-mean Nusselt number downstream of the leading edge is found to be located in the region of the peak vertical thermal eddy diffusivity and

the time-mean point of reattachment of the separating streamline. The profile of the local time-mean Nusselt number compares well with those obtained experimentally at higher Peclet numbers. Vortex action in drawing cooler fluid towards the plate surface leads to instantaneous local peaks in the Nusselt number along the plate surface; a prominent peak is located at the point of reattachment.

Acknowledgements

M.C. Thompson gratefully acknowledges the support of a CSIRO Postdoctoral Fellowship Award. The computing was supported by a CSIRONET Cyber 205 Grant.

Nomenclature

C_p	heat capacity of fluid at constant pressure
D_v	vertical thermal eddy diffusivity $[-\overline{v'T'}/(\partial\bar{T}/\partial y)]$
H	semi-thickness of plate
$i \equiv \sqrt{-1}$	
k	thermal conductivity of fluid
Nu	Nusselt number $[-\partial(T/\Delta T)/\partial(y/2H)]_{y=0}$
$\overline{Nu}$	time-mean Nusselt number
$\overline{Nu}_{max}$	maximum value of $\overline{Nu}$ occurring near reattachment
Pe	Peclet number $C_p \rho V_\infty 2H/k$
t	time
T	temperature of fluid
T_o	temperature of unheated fluid
T_1	temperature at plate surface
V'	fluctuation of vertical velocity
$\underline{u}$	fluid velocity normalized to V_∞
V_∞	magnitude of velocity of flow at upstream infinity
x	horizontal coordinate direction
x_R	reattachment length
y	vertical coordinate direction
$z \equiv x+iy$	complex coordinate in physical plane
λ	complex coordinate in transformed plane
ΔT	temperature difference between plate and incident fluid
ϕ	complex flow velocity potential
ρ	fluid density
τ	dimensionless time $tV_\infty/2H$

References

1. V.T. Morgan, Advances in Heat Transfer, 11, Academic Press, New York (1975).
2. A.M. Gooray, C.B. Watkins and W. Aung, J. Heat Transfer, Trans. ASME, 107, 70 (1985).
3. E.M. Sparrow and J.E. O'Brien, J. Heat Transfer, Trans. ASME, 102, 408 (1980).
4. T. Ota and N. Kon, J. Heat Transfer, Trans. ASME, 96, 459 (1974).
5. R.L. Zelenka and R.I. Loehrke, J. Heat Transfer, Trans. ASME, 105, 172 (1983).
6. P.I Cooper, J.C. Sheridan and G.J. Flood, Int. J. Heat and Fluid Flow 7, 61 (1986).
7. D.C. McCormick, R.C. Lessmann and F.L. Test, J. Heat Transfer, Trans. ASME, 106, 276 (1984).
8. D.G. Motwani, U.N. Gaitonde and S.P. Sukhatme, J. Heat Transfer, Trans. ASME, 107, 307 (1985).
9. M. Kiya and K. Sasaki, Proc. 5th Symp. on Turbulent Shear Flows, Cornell University, Ithaca, New York, 5.7 (1985).
10. M. Kiya, K. Sasaki and M. Arie, J. Fluid Mech. 120, 219 (1982).
11. S. Nagano, M. Naito and H. Takata, Computers and Fluids 10, 243 (1982).
12. B.R Morton, Geophys. Astr. Fluid Dynamics 86, 277 (1984).
13. R. Hillier and N.J. Cherry, J. Wind Engng. Ind. Aerodyn. 8, 49 (1981).
14. B.P. Leonard, Computer Methods in Applied Mechanics and Engineering 19, 59 (1979).
15. C.E. Leith, Methods in Comp. Phys. 4, 1 (1965).
16. P.H. Rothe and J.P. Johnston, J. Fluids Engineering, Trans. ASME, 101, 117 (1979).